Impact of anthropogenic heat emissions on meteorological parameters and air quality in Beijing using a high-resolution model simulation

Hengrui Tao[1,2,3], Jia Xing(⌧)[2,3], Gaofeng Pan[1], Jonathan Pleim[4], Limei Ran[5], Shuxiao Wang[2,3], Xing Chang[2,3], Guojing Li[6], Fei Chen[7], Junhua Li(⌧)[2,3]

1 Aviation University of Air Force, Changchun , 130022, China

2 School of Environment and State Key Joint Laboratory of Environment Simulation and Pollution Control, Tsinghua University, Beijing, 100084, China

3 State Environmental Protection Key Laboratory of Sources and Control of Air Pollution Complex, Beijing, 100084, China

4 Research Triangle Park, Environmental Protection Agency, NC, 27711, USA

5 East Remote Sensing Laboratory, United States Department of Agriculture, NC, 20250, USA

6 Unit No.96941 of Chinese People's Liberation Army, Beijing, 100041, China

7 Unit No.31010 of Chinese People's Liberation Army, Beijing, 100081, China

⌧Corresponding authors

E-mail: xingjia@tsinghua.edu.cn (J. Xing); lijunhua@tsinghua.edu.cn (J. Li)

S1. LUCY modifying

We made three modifications to ensure that the model assumptions are closer to the reality in Beijing. First, the migrant population was not considered in LUCY and so we incorporated it into the total population and it was calculated by the following function:

$$P = P_C + P_L$$

Where P_C is the resident population and P_L is the migrant population. Second, the number of heating degree days (HDD) and cooling degree days (CDD) was very important to the calculation of energy consumption. We updated it by applying the daily air temperature data of China meteorological data network to the LUCY. Third, the metabolic rate of Asian was different from the European. We recalculated the metabolic rate with specific population characteristics such as age demographics and lifestyle in Beijing. The detail are as follows.

The metabolic rates γ_N at night (sleeping) and γ_D during daytime (remaining activities) are:

$$\gamma_N = M_1 \sum_{j=1}^{8} (f_{R,j} A_j \frac{P_j}{P_{tot}}) \quad \text{(S1)}$$

$$\gamma_D = \sum_{j=1}^{8} \left(f_{R,j} A_j \frac{P_j}{P_{tot}} \sum_{i=2}^{10} (\frac{t_{ji}}{24 - t_{1i}} M_i) \right) \quad \text{(S2)}$$

The resident population P is divided into eight age groups; time t is distributed by each group in different activities (ten classes) ; standard metabolic rates M (W m^{-2} of body surface area) of a standard person (30 years old, average body) for each activity (ISO 8996, 2004); age correction factors f_R to account for variation of M with age (Altman and Dittmer, 1968) and mean body surface area A for each age group (Mosteller, 1987) and A is calculated as average for males and females by assuming a 1:1 male-to-female ratio. Index j refers to the eight age groups, index i covers the ten specific activities (i =1 for sleeping). The above data are in Table S1.

More information about LUCY can refer to Lindberg et al., 2013, Impact of city changes and weather on anthropogenic heat flux in Europe 1995-2015; Allen et al., 2011, Global to city scale model for anthropogenic heat flux.

S2. Model coupling

i) For matching the WRF simulation, the format of LUCY output data was processed by using the ArcGis and Spatial Allocate tools.

ii) According to the Eq. (S3), the AHE is allocated to the sensible heat flux of Pleim-Xiu land surface model.

$$SH = F_V \cdot SH_V + F_U \cdot (SH_U + Q_{F \cdot S}) \qquad \text{(S3)}$$

The SH is total sensible heat flux in the unit grid. SH_v and F_v are the vegetation sensible heat flux and vegetation fraction in the unit grid. SH_u and F_u are the urban sensible heat flux and urban fraction in the unit grid.

iii) Detailed coupling processes

a. In the Registry.EM_COMMON program of Registry directory, we added new parameters - AHEEAT, lucy_AHEeat_in, lucy_update_hour, etc, which was related to the AHE flux.

b. Modified the module_first_rk_step_part1.F program in dyn_em directory.

c. Modified the main program - module_sf_pxlsm.F of Pleim-Xiu land surface scheme in the directory of phys and corresponding driver layer program - module_surface_driver.F.

d. Modified the user selection card text of namelist.input in the directory of run.

S3. Model evaluation

S3.1. Meteorological parameters

The sixteen common observation stations (marked as green symbols in Fig. S1) in Domain 4, which derived from China National Environmental Monitoring Center, were used to do statistic analysis, with 3-h intervals and more than 95% valid records at these meteorological stations. Due to the limited observational data available, the statistical evaluations were restricted to the 2 m temperature (T_2), 10 m wind speed (WS_{10}). The performance of WRF model was evaluated based on four statistical metrics including mean bias (MB), root mean square error (RMSE), Pearson correlation coefficient (R), and index of agreement (IOA).

Table S2 presents the statistical results between simulation and corresponding meteorological observation. For T_2, the performances of AHE_1km in the urban stations were better than noAHE_1km. Especially in December, the mean of MB, R, RMSE, IOA were -0.58 ℃, 0.87, 2.24 ℃, 0.87 in AHE_1km, significantly better than the value in noAHE_1km (-1.04 ℃, 0.85, 2.7 ℃, 0.84). And in some stations with high AHE (eg. BJ, TJ), the simulated improvement was more obvious. In July, the MB in AHE_1km had a little bit bigger, but the performances of R and IOA were better than noAHE_1km. In contrast, in the suburban stations, the AHE is small and the differences between noAHE_1km and AHE_1km was nearly negligible no matter in Dec or July. For WS_{10}, the effect of AHE was little due to its variability and the performances of noAHE_1km and AHE_1km were nearly at a similar level. In December, the mean of MB and R were respectively 0.08, 0.14 m s^{-1} and 0.68, 0.69 in noAHE_1km and AHE_1km; In July, due to more variable wind, they were 0.15, 0.2 m s^{-1} and 0.44, 0.45.

Meanwhile, Fig. S2 shows that time series of T_2 in AHE_1km is more consistent with observed data than noAHE_1km. The time series of WS_{10} in both noAHE_1km and AHE_1km had some deviations from the observation to some extent, but overall they were consistent.

In summary, the above illustrated that both AHE_1km and noAHE_1km can well capture the temporal variations and magnitudes of T_2 and WS_{10}, and generally the model performance of AHE_1km was more accurate and suitable than noAHE_1km.

S3.2. Air quality

The observed data are derived from the China National Environmental Monitoring Center at 35 air-quality stations marked as red triangles in Fig. S1. Table S3 summarizes the statistical results of model performance in simulating $PM_{2.5}$ and O_3 including normalized mean bias (NMB), normalized mean error (NME), mean fractional bias (MFB), and mean fractional error (MFE).

In AHE_1km and noAHE_1km, the MFB and MFE of $PM_{2.5}$ were respectively within ±35.1, ±53.7%; the MFB and MFE of O_3 were respectively within ±33.2, ±49.2% (Table S3). The relatively larger biases in summer $PM_{2.5}$ and winter O_3 might be associated with the corresponding low $PM_{2.5}$ and O_3 concentrations, when the influence from model uncertainties became relatively larger than in other months. Overall, the simulated performances of air quality met the criteria for air pollutants proposed by Boylan and Russell (2007) and EPA (2007) - in which both the MFE and the MFB were suggested to be no greater than ±75 % and ±60 %, respectively. Moreover, the variation tendency of $PM_{2.5}$, O_3 in their pollution seasons were generally consistent with observed data (Fig. S3) and the R were above 0.64 and 0.7, respectively.

The above statistics of meteorological parameters and air quality illustrated that model performance of WRF-CMAQ were acceptable.

Tables and Figures

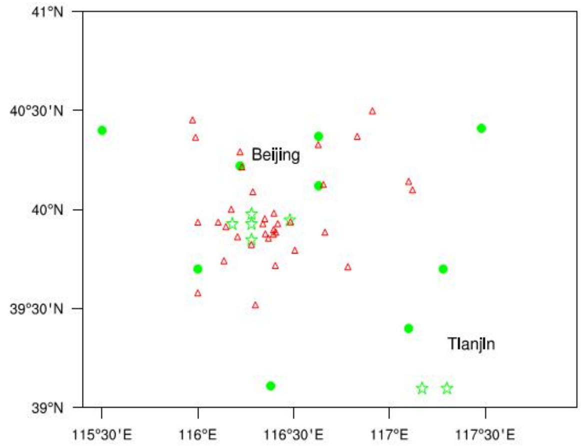

Figure S1. The distribution of meteorological observation sites (green) and air quality observation sites (red) in the WRF-CMAQ innermost simulation domain

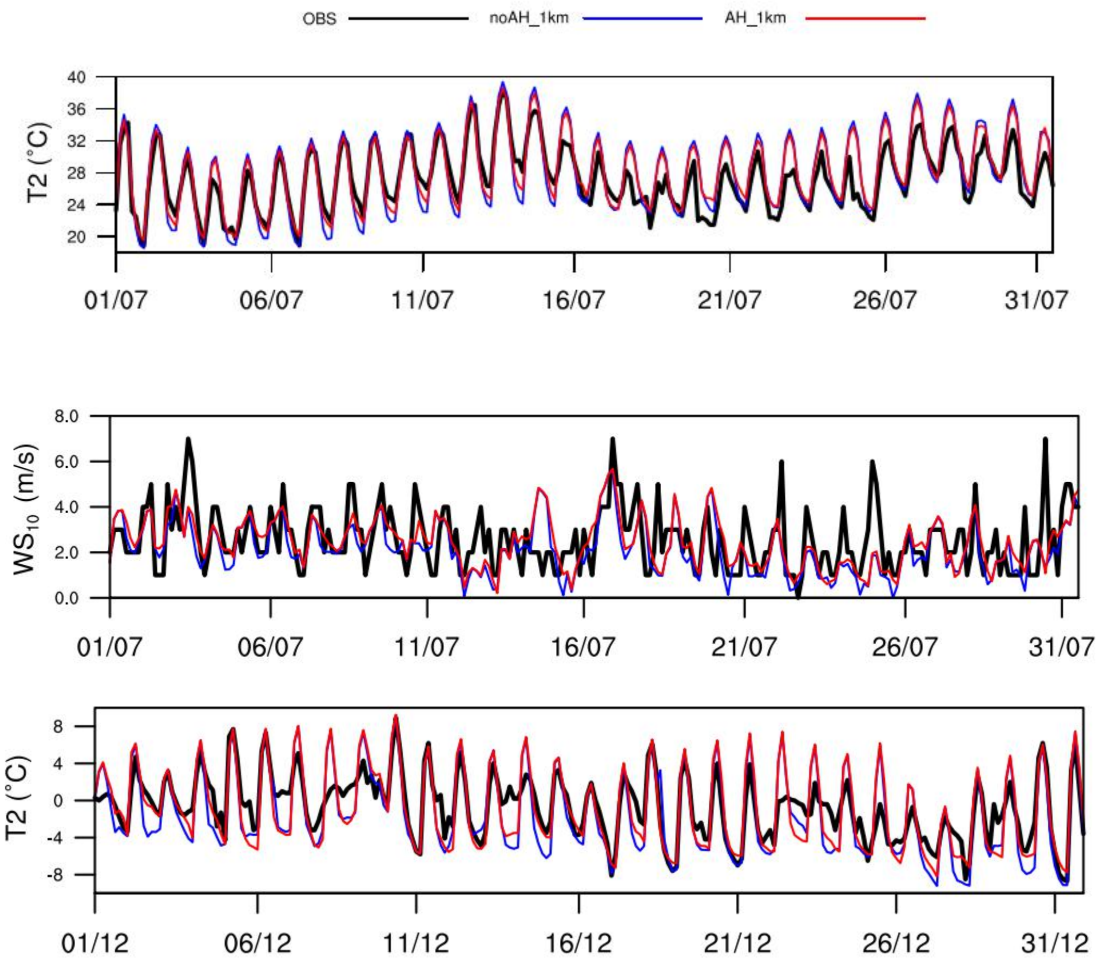

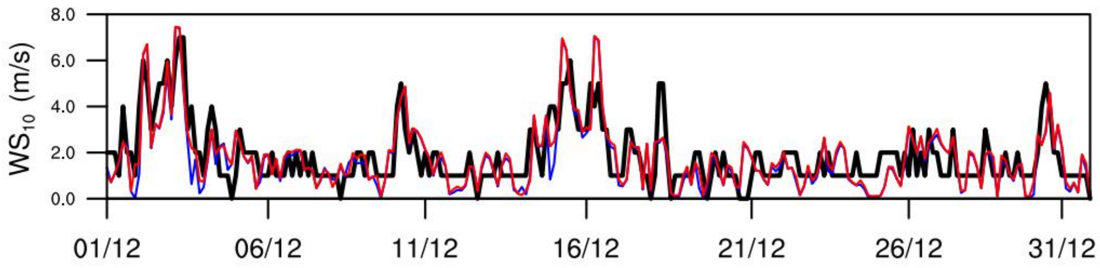

Figure S2. Time series of T_2 and WS_{10} in green marked meteorological stations for July and December

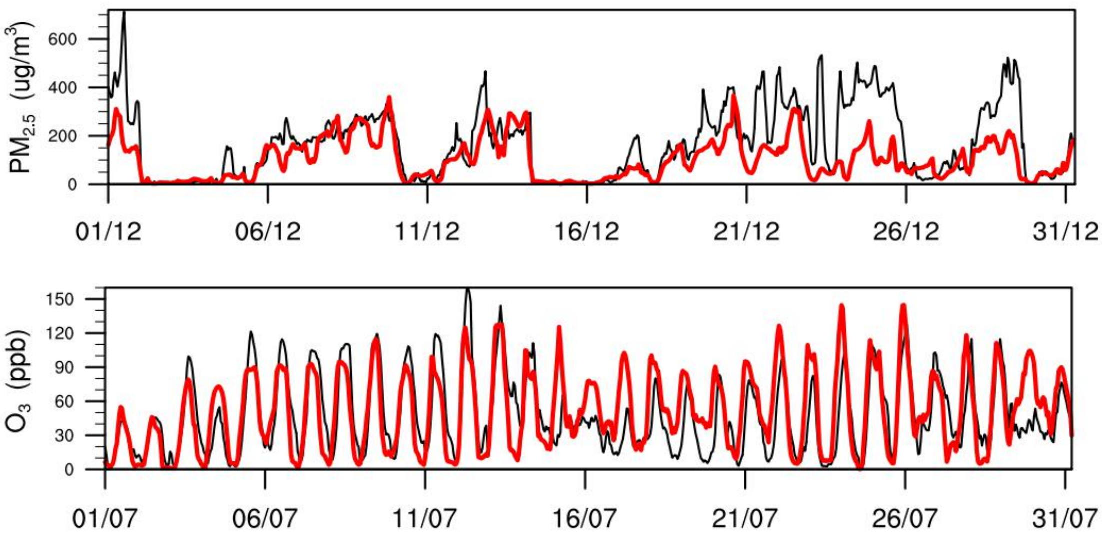

Figure S3. Time series of monthly $PM_{2.5}$ in December and O_3 in July of red marked stations

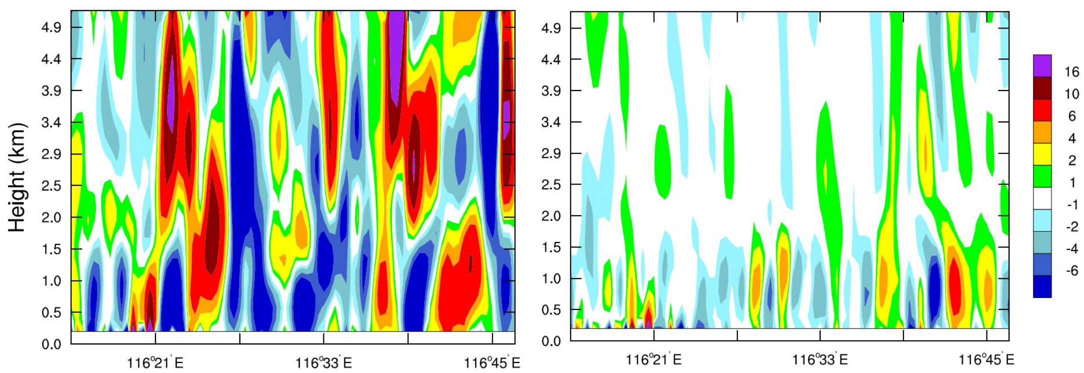

Figure S4. Vertical profile of ΔW (mm s^{-1}) along the line connecting two points in July (One is the northwest point of Beijing-urban, which is located in the 40°N, 116°15’E. The other point is located in 39°40’N,116°47’E, which is along with the diagonal line of Beijing-urban and extended to Beijing-Tianjin border. Left: local thermal convective showers, right : systematic continuous precipitation)

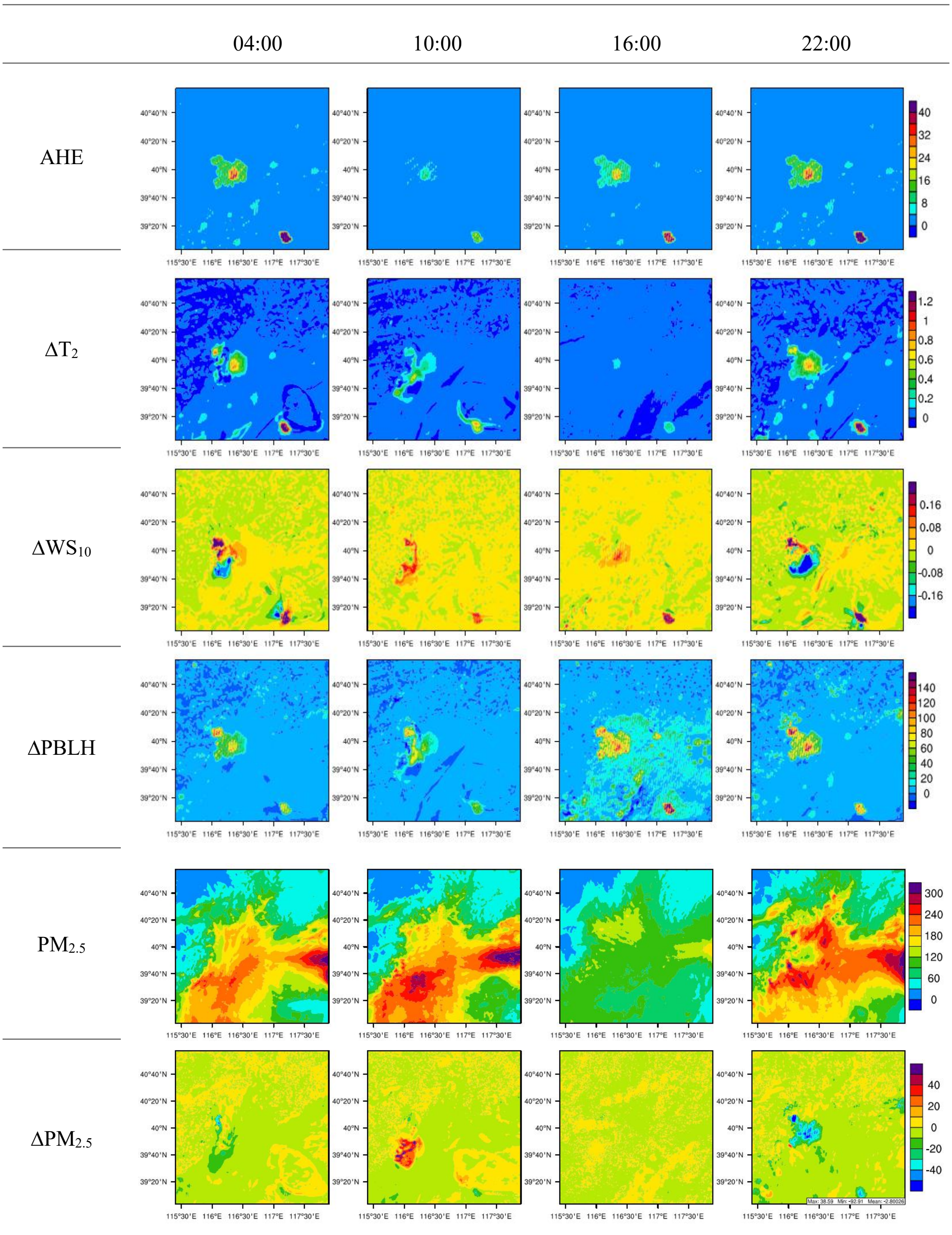
04:00
10:00
16:00
22:00
AHE
ΔT_2
ΔWS_{10}
$\Delta PBLH$
$PM_{2.5}$
$\Delta PM_{2.5}$

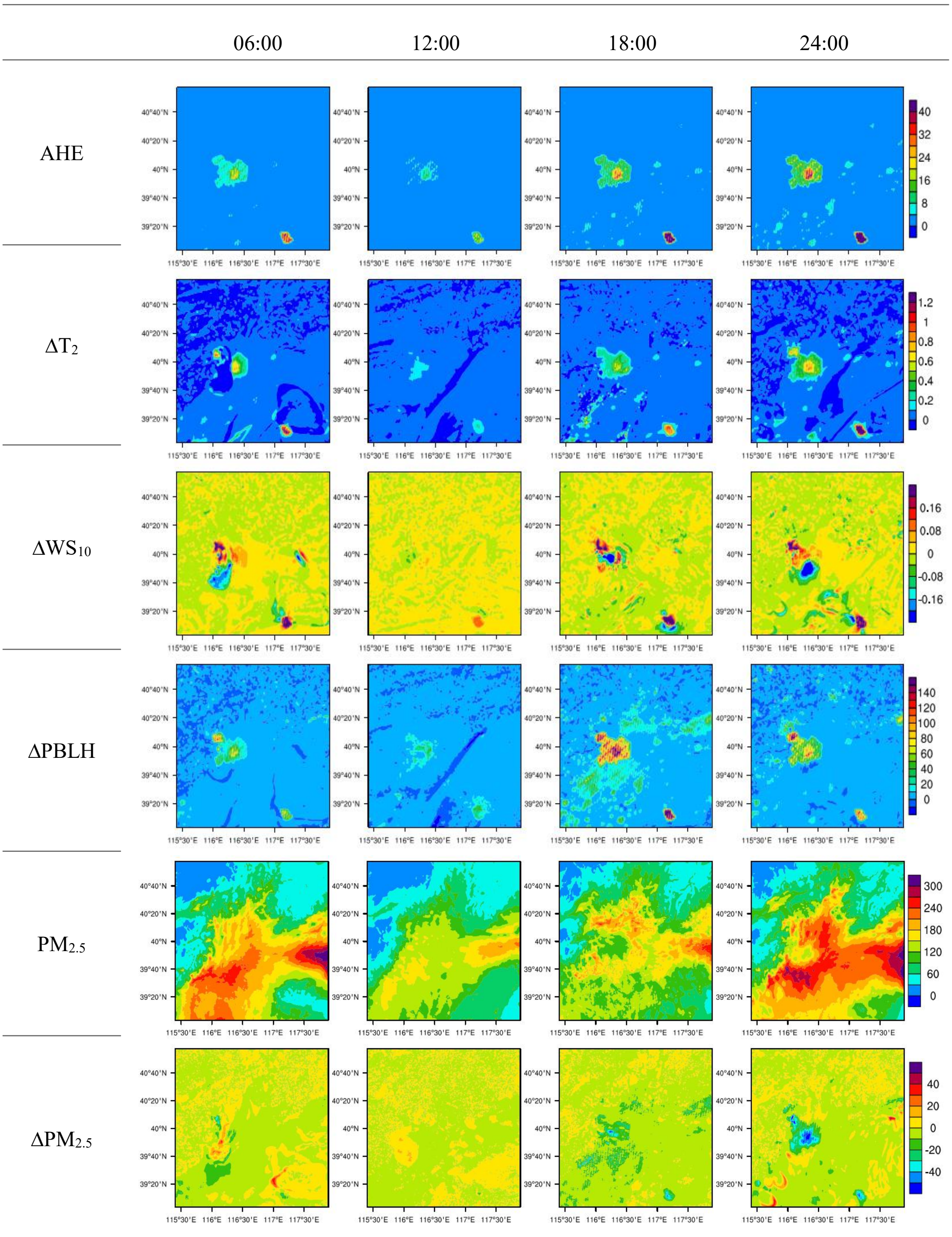

Figure S5. Spatial distribution of AHE, ΔT_2, ΔWS_{10}, $\Delta PBLH$, $PM_{2.5}$, and $\Delta PM_{2.5}$ during a heavy pollution period at 04:00,10:00,16:00,22:00,06:00,12:00,18:00,24:00

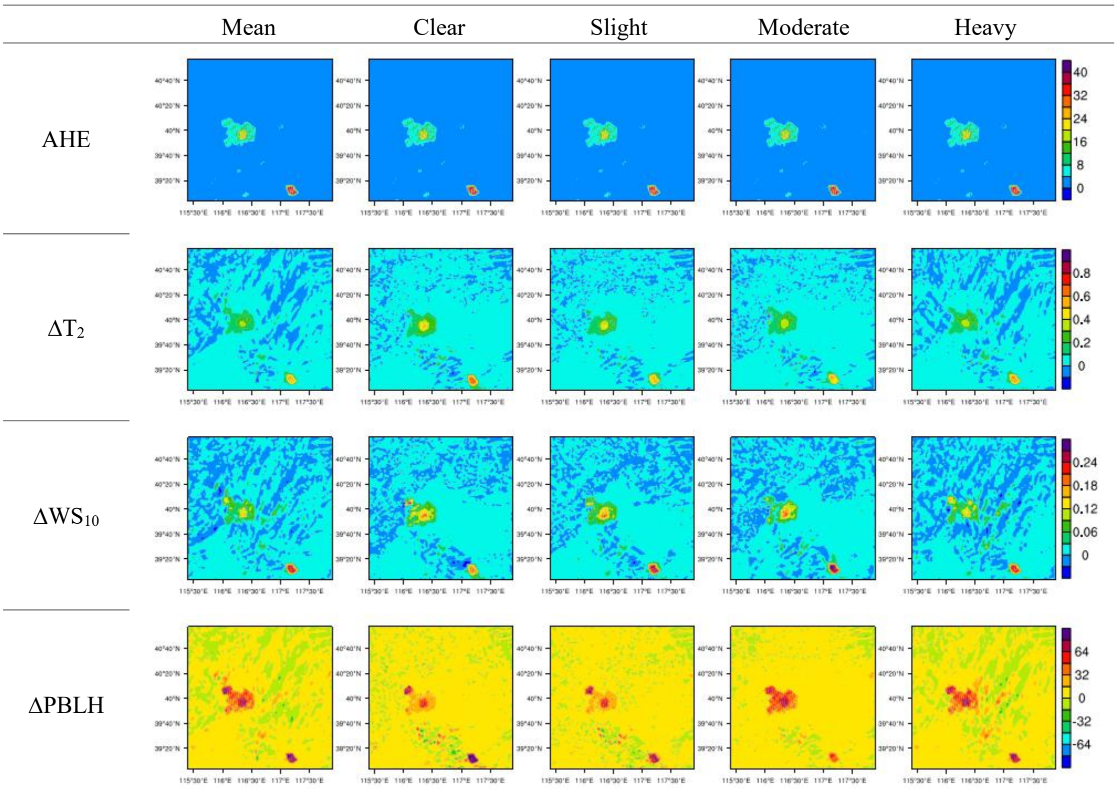

Figure S6. Spatial distribution of AHE, ΔT_2, ΔWS_{10}, and ΔPBLH at monthly averaged level and across different O_3 pollution levels

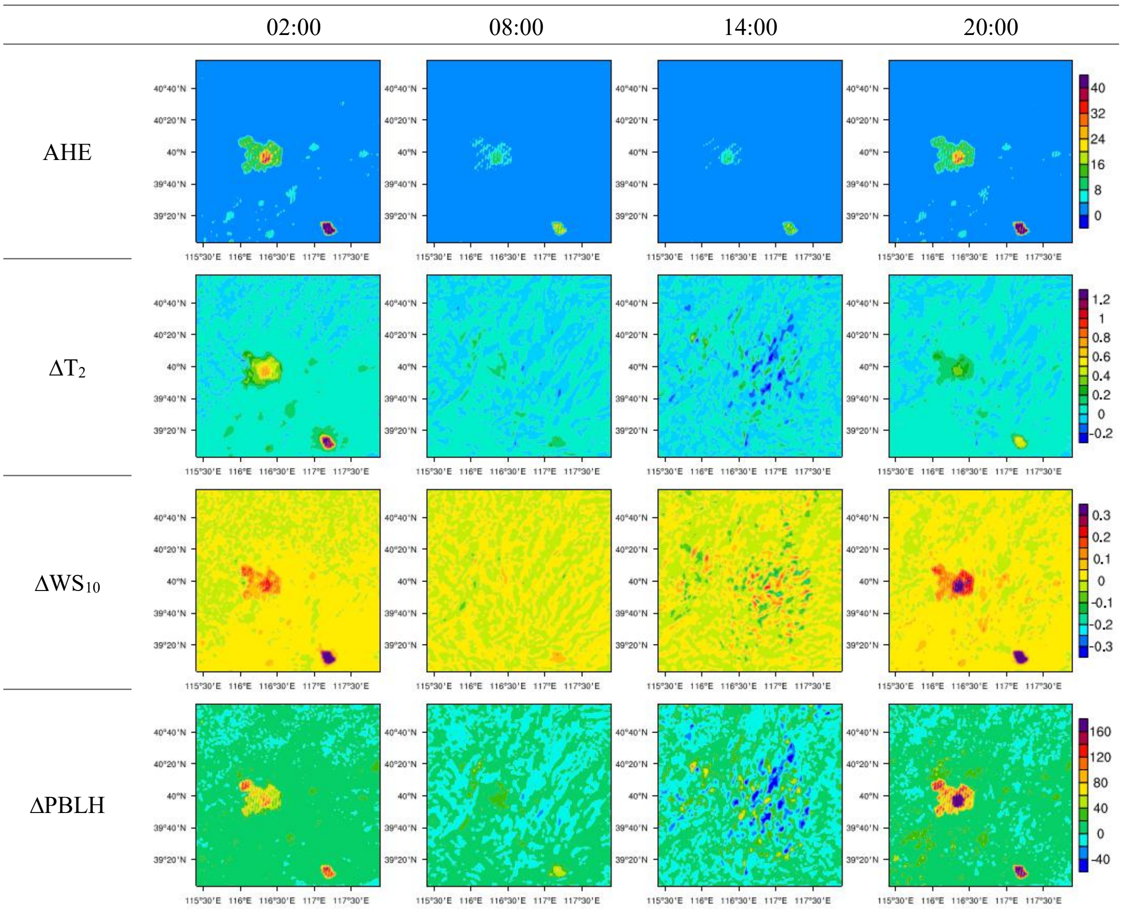

Figure S7. Spatial distribution of AHE, ΔT_2, ΔWS_{10}, $\Delta PBLH$ at 02:00, 08:00, 14:00, 20:00 in July

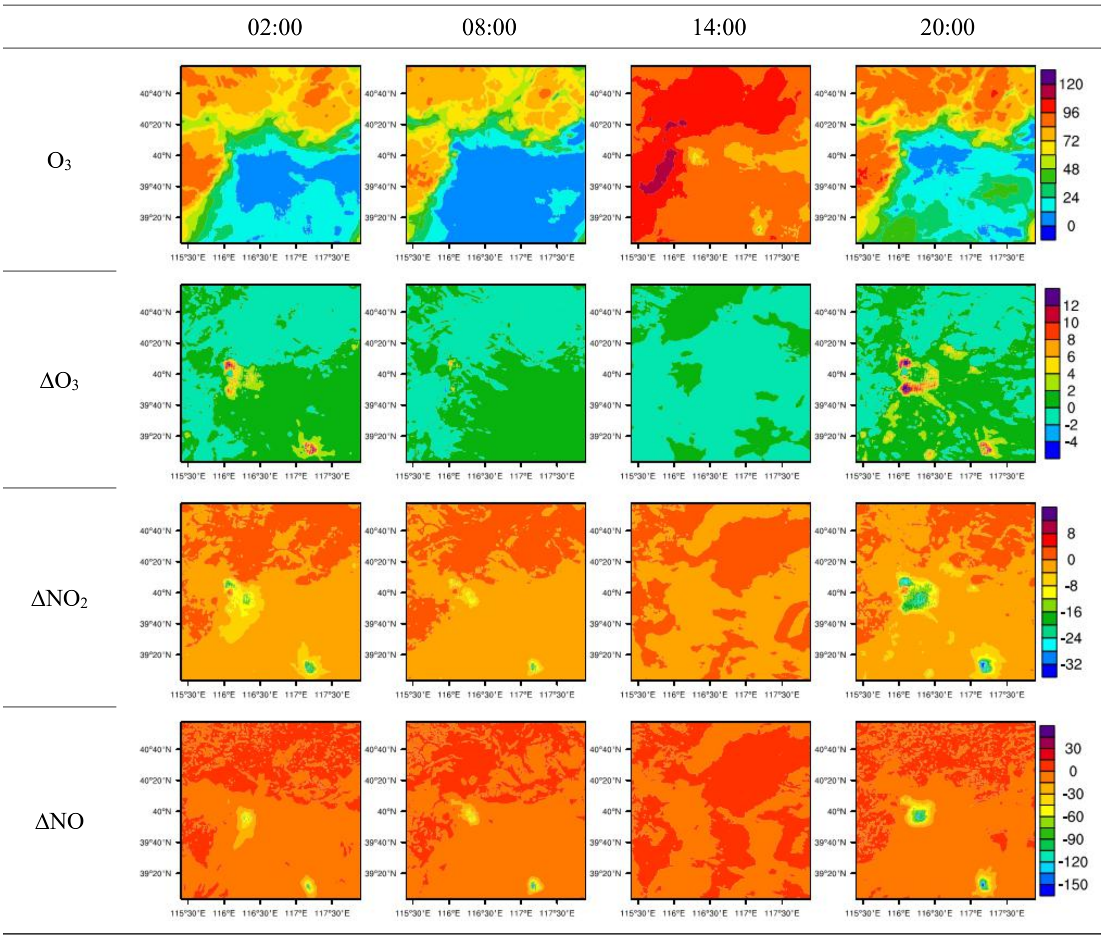

Figure S8. Spatial distribution of O_3, ΔO_3, ΔNO_2, ΔNO at 02:00, 08:00, 14:00, 20:00 in July

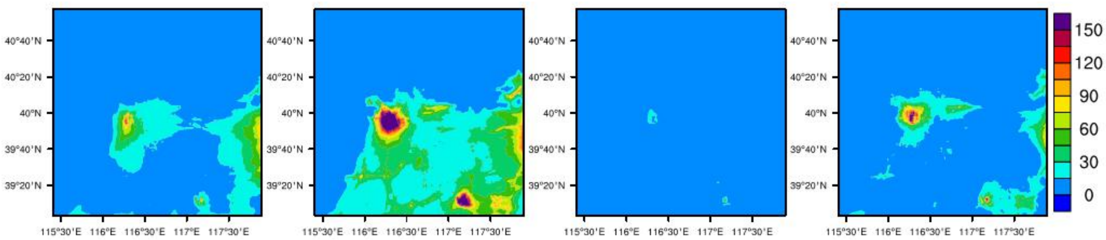

Figure S9. Spatial distribution of NO at 02:00, 08:00, 14:00, 20:00 in July (left to right)

Table S1. Data in Beijing used to calculate the average metabolic rate

Age	0-4	5-14	15-19	20-24	25-44	45-59	60-79	≥80	
Persons	1409	2614	1231	1597	7790	3427	2765	7081	
Activity					Time（h）				M（W m^{-2}）
Sleep	13	10	9	8.5	8	8	8.5	9	40
Sitting ,at rest	3	2	1	0.5	0.5	1	2.5	7	55
Standing,at rest	1	1	0.5	0.5	0.5	0.5	1	1	70
Sitting, light activity	3	4	4.5	5	5	5	4.5	4.5	70
Standing, light activity	2	3.5	3	3.5	3.5	3	3	1	93
Standing, medium activity	1	2	2	2	2	2	2	0.5	116
Walking on the level	1	1	2	2	2	1.5	1.5	1	140
Walking uphill, ladder, etc.	0	0.5	1	1	1	1	0.5	0	200
Hard work	0	0	0.5	1	1	1	0.5	0	230
Very hard work, sport	0	0	0.5	0.5	0.5	0.5	0	0	290
f_R (-)	1.31	1.10	1.08	1.03	1.00	0.97	0.92	0.89	
A（m^2）	0.5	1.07	1.5	1.7	1.8	1.8	1.75	1.7	

Table S2a. Statistical results of T_2, WS_{10} between noAHE_1km (C1), AHE_1km (C2) and observed data in July (MO is the mean of observed values. Superscript word ”1” and ”2” respectively represent urban and suburban stations. The same as below.)

	July																	
	T_2 (ºC)									WS_{10} (m s^{-1})								
	Value			R		RMSE		IOA		Value			R		RMSE		IOA	
	MO	C1	C2	C1	C2	C1	C2	C1	C2	MO	C1	C2	C1	C2	C1	C2	C1	C2
BJ[1]	26.9	27.3	27.5	0.9	0.91	2.7	2.7	0.9	0.9	2	1.74	1.81	0.44	0.44	1.1	1.1	0.65	0.65
FT[1]	28.1	28.9	29	0.9	0.9	1.7	1.7	0.87	0.87	1.55	1.82	1.86	0.41	0.41	0.81	0.81	0.62	0.62
DX[1]	28	28.9	28.9	0.92	0.92	1.7	1.7	0.87	0.87	1.53	1.93	1.93	0.49	0.51	0.9	0.9	0.67	0.68
TJ[1]	27.3	27.8	28.1	0.88	0.9	2.5	2.1	0.9	0.93	2.56	2.17	2.46	0.48	0.47	1.32	1.27	0.68	0.69
BC[1]	26.6	27.2	27.5	0.87	0.88	2	2	0.89	0.89	1.62	2.28	2.45	0.52	0.53	1.1	1.1	0.65	0.64
SJS[1]	27.7	28.7	28.7	0.89	0.89	2.1	2.1	0.86	0.86	1.13	1.83	1.83	0.36	0.37	0.88	0.88	0.68	0.69
SY[2]	27.4	28.5	28.5	0.88	0.88	2.1	2.1	0.82	0.82	1.76	1.87	1.88	0.48	0.49	0.76	0.75	0.68	0.69
HR[2]	27.1	27.8	27.8	0.88	0.88	1.8	1.8	0.87	0.87	1.58	1.79	1.78	0.38	0.38	0.93	0.92	0.64	0.64
CP[2]	27.3	28.1	28.1	0.86	0.86	2.1	2.1	0.83	0.83	1.53	1.63	1.64	0.41	0.41	0.86	0.86	0.66	0.66
FS[2]	27.5	28.6	28.6	0.9	0.9	2	2	0.83	0.83	2.22	1.86	1.86	0.5	0.5	1.1	1.1	0.66	0.66

Table S2b. Statistical results of T_2, WS_{10} between C1, C2 and observed data in Dec

	December																	
	T_2 (ºC)									WS_{10} (m s^{-1})								
	Value			R		RMSE		IOA		Value			R		RMSE		IOA	
	MO	C1	C2	C1	C2	C1	C2	C1	C2	MO	C1	C2	C1	C2	C1	C2	C1	C2
BJ[1]	0.18	-0.63	-0.24	0.82	0.84	4.1	3.7	0.78	0.8	1.84	1.73	1.83	0.73	0.74	1	0.98	0.85	0.86
HD[1]	0.43	-0.61	-0.26	0.87	0.88	2.1	1.6	0.88	0.91	1.7	2.17	2.19	0.77	0.77	0.8	0.8	0.82	0.82
CY[1]	0.7	-0.35	0.22	0.85	0.88	1.85	1.3	0.88	0.93	1.97	2.1	2.24	0.69	0.73	0.95	0.91	0.82	0.84
FT[1]	1.04	-0.16	0.18	0.84	0.85	2.6	2.4	0.82	0.84	1.72	1.91	1.92	0.77	0.77	0.83	0.83	0.87	0.87
DX[1]	0.18	-0.81	-0.78	0.85	0.86	2.3	2.3	0.85	0.85	1.39	1.9	1.89	0.7	0.71	0.92	0.92	0.78	0.79
TJ[1]	0.12	-1.16	-0.05	0.87	0.89	3.5	1.9	0.82	0.91	2.15	1.84	2.14	0.84	0.84	0.94	0.89	0.84	0.9
BC[1]	-0.72	-1.4	-0.93	0.86	0.86	2.49	2.27	0.9	0.91	1.78	1.95	2.23	0.77	0.77	0.94	1	0.87	0.86
SJS[1]	1.02	-0.3	0.15	0.85	0.86	2.6	2.5	0.81	0.83	1.23	1.65	1.68	0.53	0.53	1.1	1.1	0.61	0.61
SY[2]	0	-1.15	-1.1	0.88	0.88	2.2	2.3	0.85	0.85	1.81	1.99	1.99	0.74	0.74	0.96	0.96	0.84	0.84
HR[2]	-1.1	-1.68	-1.67	0.85	0.85	1.75	1.75	0.9	0.9	1.78	1.72	1.72	0.51	0.51	1	1	0.71	0.71
CP[2]	0.43	-0.53	-0.49	0.82	0.82	2.2	2.2	0.84	0.84	1.93	2.1	2.1	0.5	0.5	1	1	0.71	0.71
FS[2]	0	-0.92	-0.91	0.84	0.84	2.4	2.4	0.84	0.85	2.29	1.45	1.44	0.66	0.66	1.2	1.2	0.72	0.72

Table S3. Statistical results of monthly $PM_{2.5}$, O_3 in July and Dec between C1, C2 and observed data

	July				December			
	$PM_{2.5}$		O_3		$PM_{2.5}$		O_3	
	C1	C2	C1	C2	C1	C2	C1	C2
NMB(%)	-25.8	-27.7	15.2	16.4	-22.7	-23.2	24.3	28.5
NME(%)	34.5	36.2	24.3	22.4	48.5	47.4	38.2	39.7
MFB(%)	-23.3	-26.8	20.7	21.5	-35.1	-34.5	31.5	33.2
MFE(%)	51.5	53.7	35.6	33.5	41.1	42.7	45.4	49.2
R	0.42	0.41	0.7	0.71	0.64	0.64	0.5	0.49

Table S4. Simulated mean in T_2 and WS_{10} across the noAHE_1km, AHE_1km, noAHE_3km, and AHE_3km scenarios compared with observed data in December of 2015

	T_2 (ºC)					WS_{10} (m s^{-1})				
	MO	**noAHE_1km**	**AHE_1km**	**noAHE_3km**	**AHE_3km**	**MO**	**noAHE_1km**	**AHE_1km**	**noAHE_3km**	**AHE_3km**
BJ[1]	0.18	-0.63	-0.24	-0.57	-0.57	1.84	1.73	1.83	1.96	1.96
HD[1]	0.43	-0.61	-0.26	-0.53	-0.53	1.7	2.17	2.19	2.13	2.13
CY[1]	0.7	-0.35	0.22	-0.55	-0.55	1.97	2.1	2.24	2.35	2.35
FT[1]	1.04	-0.16	0.18	-0.26	-0.26	1.72	1.91	1.92	2.11	2.11
DX[2]	0.18	-0.81	-0.78	-0.89	-0.89	1.39	1.9	1.89	2.18	2.18
TJ[1]	0.12	-1.15	-0.05	-1.21	-1.21	2.15	1.84	2.14	1.89	1.89
BC[1]	-0.72	-1.4	-0.93	-1.36	-1.36	1.78	1.95	2.23	2.01	2.01
SJS[1]	1.02	-0.3	0.15	-0.23	-0.23	1.23	1.65	1.68	1.91	1.91
SY[2]	0	-1.15	-1.1	-1.1	-1.1	1.81	1.99	1.99	2.33	2.33
HR[2]	-1.1	-1.68	-1.67	-1.56	-1.56	1.78	1.72	1.72	2.02	2.02
CP[2]	0.43	-0.53	-0.49	-0.61	-0.61	1.93	2.1	2.1	2.3	2.3
FS[2]	0	-0.92	-0.91	-0.96	-0.96	2.29	1.45	1.44	1.62	1.62
B1	0.24	-0.58	0.71	-0.55	0.03	1.89	1.77	2.08	1.94	2.15
B2	0.15	-0.69	0.42	-0.73	-0.31	1.76	1.92	2.18	1.88	2.06

Table S5. Concentration criteria under different $PM_{2.5}$ pollution levels

(Variable "a" represents the concentration of $PM_{2.5}$.)

Levels	Clean(I)	Moderate clean(II)	Slight pollution(III)	Moderate pollution(IV)	Heavy pollution(V)	Severe pollution(VI)
Concentration (μg m^{-3})	a<35	35≦a<75	75≦a<115	115≦a<150	150≦a<250	250≦a

Table S6. Concentration criteria under different O_3 pollution levels.

(Variable "a" represents the average of daily maximum 8h O_3.)

Levels	Clean(I)	Slight pollution(II)	Moderate pollution(III)	Heavy pollution(IV)
Concentration(ppb)	a<40	40≦a<50	50≦a<80	80≦a

References

Altman P L, Dittmer D S (1968). Metabolism. Federation of American Societies for Experimental Biology: Bethesda, Maryland

Boylan J W, Russell A G (2007). PM and light extinction model performance metrics, goals, and criteria for three-dimensional air quality models. Atmospheric Environment, 40(26):4946-59

EPA (2007). Guidance on the Use of Models and Other Analyses for Demonstrating Attainment of Air Quality Goals for Ozone, $PM_{2.5}$, and Regional Haze. In: EPA, editor

ISO 8996 (2004). Ergonomics of the Thermal Environment - Determination of Metabolic Heat Production. International Organization for Standardization: Geneva, Switzerland

Mostller R D (1987). Simplified calculation of body surface area. New England Journal of Medicine, 317:1098-1098